



OPEN

# Modified surface plasmon polaritons for the nanoconcentration and long-range propagation of optical energy

Huawei Liang, Shuangchen Ruan, Min Zhang, Hong Su & Irene Ling Li

SUBJECT AREAS:

NANOPHOTONICS AND  
PLASMONICS

SUB-WAVELENGTH OPTICS

Received  
20 January 2014

Accepted  
2 May 2014

Published  
20 May 2014

Correspondence and  
requests for materials  
should be addressed to  
H.W.L. (hwliang@szu.  
edu.cn) or S.C.R.  
(scruan@szu.edu.cn)

<sup>1</sup>College of Electronic Science and Technology, Shenzhen University, Shenzhen, 518060, China, <sup>2</sup>Shenzhen Key Laboratory of Laser Engineering, Shenzhen University, Shenzhen, 518060, China, <sup>3</sup>Key Laboratory of Advanced Optical Precision Manufacturing Technology of Guangdong Higher Education Institutes, Shenzhen University, Shenzhen, 518060, China.

We propose a new surface plasmon polariton concept for the nanoconcentration and long-range propagation of optical energy. The propagation loss from the mode can be greatly decreased, and the mode nanoconfinement can be simultaneously maintained, by appropriately modifying the field distribution of the surface plasmon polaritons. Furthermore, we present a metal nanowire placed in a dielectric hole to guide the mode and achieve both a 26 nm beam radius and a 24 mm propagation distance. We expect the modified surface plasmon polaritons to motivate many important applications in nanophotonics, biophotonics, and highly integrated photonic circuits.

Surface plasmon polaritons<sup>1,2</sup> have great prospects in the field of nanophotonics<sup>3</sup> for mode nanoconfinement, but their propagation losses are very high<sup>4–10</sup>. For typical SPP waveguides, the propagation losses mainly result from the electromagnetic fields inside the metal. Long-range (LR) SPPs can significantly reduce propagation losses, but their mode confinement is only comparable to that of conventional dielectric waveguides<sup>11–15</sup>. The hybrid modes propagating on a metal surface separated from a dielectric nanowire can guide light far beyond the diffraction limit; however, the propagation distances are typically shorter than those of SPPs propagating along an equivalent air-metal interface<sup>16–19</sup>.

In this paper, we propose a new concept of modified surface plasmon polaritons (MSPPs) for the deep sub-wavelength and low-loss propagation of optical energy. For the MSPPs, the optical power inside the metal can be significantly reduced by modifying a part of the mode fields of the SPPs, dramatically decreasing propagation losses. At the same time, the mode nanoconfinement can be maintained by keeping the other part of the mode fields nearly unchanged. For example, the light can travel over 24 mm with a 26 nm beam radius using MSPPs on a silver nanowire placed in a silicon hole. The combination of nanoconcentration and long-range propagation makes the MSPPs particularly useful for the future design and development of sub-wavelength devices, such as nanolasers<sup>20–22</sup>, optical nano-tweezers<sup>23,24</sup>, and nano-imaging systems<sup>25–27</sup>.

MSPPs are transverse magnetic (TM) polarised waves and can be supported by various types of waveguide structures, such as metal nanowires in dielectric holes, planar metals near dielectrics, double-coated metal nanofilms, *etc.* Here, we take a silver nanowire in a dielectric hole as an example to guide the MSPPs. When MSPPs travel on the waveguide shown in Fig. 1, the transverse magnetic field components can be written as<sup>29</sup>

$$H_{\varphi}(r) = \begin{cases} A \frac{\omega \varepsilon_1 [BJ_0(h_2 a) + N_0(h_2 a)]}{h_1 J_0(h_1 a)} J_1(h_1 r) e^{i(\omega t - \beta z)} & r < a \\ A \frac{\omega \varepsilon_2}{h_2} [BJ_1(h_2 r) + N_1(h_2 r)] e^{i(\omega t - \beta z)} & a < r < b \\ A \frac{\omega \varepsilon_3 [BJ_0(h_2 b) + N_0(h_2 b)]}{h_3 H_0^{(1)}(h_3 b)} H_1^{(1)}(h_3 r) e^{i(\omega t - \beta z)} & r > b \end{cases} \quad (1)$$

where  $\beta$  is the complex propagation constant,  $A$  is a coefficient related to the mode power, and

$$h_n = \sqrt{\varepsilon_n \left(\frac{2\pi}{\lambda}\right)^2 - \beta^2}. \quad B = \frac{\frac{\varepsilon_2 N_1(h_2 a)}{h_2 J_1(h_1 a)} - \frac{\varepsilon_1 N_0(h_2 a)}{h_1 J_0(h_1 a)}}{\frac{\varepsilon_1 J_0(h_2 a)}{h_1 J_0(h_1 a)} - \frac{\varepsilon_2 J_1(h_2 a)}{h_2 J_1(h_1 a)}}, \text{ which ensures the continuity of the transverse magnetic}$$

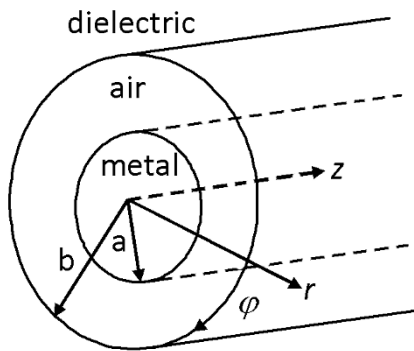


**Figure 1 | MSPP waveguide.** A silver nanowire of relative permittivity  $\epsilon_1$  and radius  $a$  is placed in the centre of a dielectric hole of relative permittivity  $\epsilon_3$  and radius  $b$ . The permittivity of silver is  $\epsilon_1 = -129 - 3.3i$  at the wavelength  $\lambda = 1550$  nm (ref. 28). The intermediate region is air, with a relative permittivity of  $\epsilon_2 = 1$ .

field components at the interface  $r = a$ .  $J_m(x)$ ,  $N_m(x)$  and  $H_m^{(1)}(x)$  are the Bessel function, the Neumann function and the Hankel function of order  $m$ .

Using the continuity of the transverse magnetic field components at the interface  $r = b$ , we obtain the following dispersion equation

$$\frac{\epsilon_2 h_3 H_0^{(1)}(h_3 b)}{\epsilon_3 h_2 H_1^{(1)}(h_3 b)} = \frac{B J_0(h_2 b) + N_0(h_2 b)}{B J_1(h_2 b) + N_1(h_2 b)} \quad (2)$$

Eq. (2) is an implicit equation in the complex variable  $\beta = \beta_1 - i\beta_2$ .  $\alpha = \beta_2$  and  $n_{\text{eff}} = \frac{\beta_1 \lambda}{2\pi}$  are the amplitude loss coefficient and effective refractive index of the MSPPs, respectively. When a silver nanowire with a radius of 10 nm is placed in a silicon hole, the dependence of  $\alpha$  and  $n_{\text{eff}}$  on the hole radius  $b$  is obtained by numerical calculation, as shown in Fig. 2. It is particularly noted that there are two zero loss points for the MSPPs, and the loss coefficient goes to zero as the hole radius tends to the two points. Therefore, one can obtain a much longer propagation distance with MSPPs than with conventional SPPs<sup>30</sup> because the loss coefficient of the SPPs on a single silver nanowire with a radius of 10 nm is  $102430 \text{ m}^{-1}$ . When the hole radius is between the two zero loss points, the MSPPs disappear because the loss coefficient is negative. When the hole radius is not between the two points, the calculation results ensure the proper decrease of the fields at infinity, so the physical validity of the MSPPs is verified.

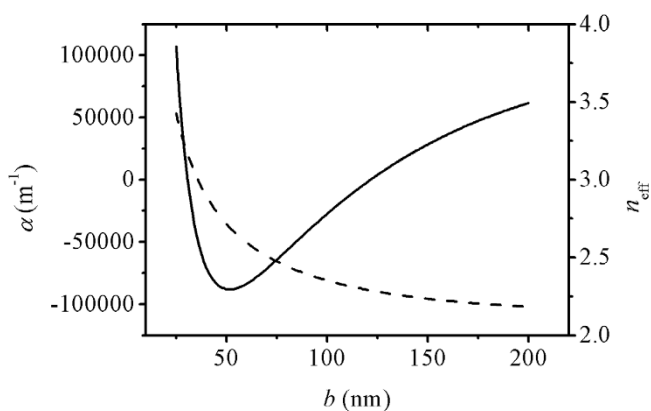


**Figure 2 | The loss coefficient (solid line) and effective refractive index (dashed line) of MSPPs guided by a silver nanowire placed in a silicon hole.** The permittivity of silicon is  $\epsilon_3 = 12.1$  at the wavelength  $\lambda = 1550$  nm (ref. 31).

When MSPPs propagate on a silver nanowire (wire radius  $a = 10$  nm) placed in a silicon hole (hole radius  $b = 121.6$  nm), the propagation constant is  $\beta = 9.28 \times 10^6 - i41.0$ , and the effective refractive index is  $n_{\text{eff}} = 2.29$ . Then, we obtain  $h_3 = 1.06 \times 10^7 + i35.8$ , and the field components are zero at infinity, so the MSPPs are still guided modes. In particular, according to Eq. (1) and the asymptotic representation of the Hankel function, the transverse magnetic field of the MSPPs can be written as

$$H_\phi(r) \approx A \frac{\omega \epsilon_3 [B J_0(h_2 b) + N_0(h_2 b)]}{h_3 H_0^{(1)}(h_3 b)} \sqrt{\frac{2}{\pi h_3 r}} e^{i(h_3 r - \frac{3\pi}{4})} e^{i(\omega t - \beta z)} \quad \text{at } |h_3 r| \gg 1,$$

so the necessary condition ensuring that the MSPPs are guided modes is  $\text{Im}(h_3) > 0$  but not  $n_{\text{eff}} > \sqrt{\epsilon_3}$ .

Based on the propagation constant above and Eq. (1), we further calculated the transverse magnetic field distribution of the MSPPs shown in Fig. 3. The field distribution of the SPPs propagating on a single silver nanowire with a radius of 10 nm is also shown for comparison. Here, we define the beam radius of the MSPPs,  $r_H$ , by the equation  $|H_\phi(r_H)| = \frac{1}{e} |H_\phi(a)|$ , which is used to define the beam radius of SPPs on a metal wire<sup>30</sup>. Using this equation, the beam radii for both the MSPPs and the SPPs are 26 nm ( $0.017\lambda$ ). However, the MSPPs' propagation distance (intensity decay by a factor of  $1/e^2$ ) is 24 nm, which is 2500 times longer than that of the SPPs. The main reason for this difference in propagation distance is their distinctive mode field distributions. When  $r < 50$  nm, the mode fields of the MSPPs and SPPs are approximately the same, so their beam radii are equal. When  $r > 50$  nm, the mode field of the MSPPs decays much more slowly than that of the SPPs, so the power proportion inside the metal for the MSPPs is much lower; accordingly, their propagation distance is much longer.

As shown in Fig. 2, when the hole radius  $b$  changes from the right zero loss point to 200 nm or from the left zero loss point to 25 nm, the loss coefficient increases considerably. However, the beam radius is almost unchanged (less than 0.5 nm). To better understand this behaviour, the transverse magnetic field distributions of the MSPPs for hole radius dimensions of  $b = 121.565$  nm (very close to the zero loss point, the black line),  $b = 160$  nm (the red line), and  $b = 200$  nm (the blue line) are shown in Fig. 4. From Fig. 4(a), one can observe that the field distributions near the nanowire are almost the same, so the beam radius is approximately constant. However, as shown in Fig. 4(a) and (b), when the hole radius goes to the zero loss point, the field distributions inside the nanowire are approximately the same, but the extension of the fields distant from the silver wire becomes larger, so the power proportion inside the silver nanowire decreases.

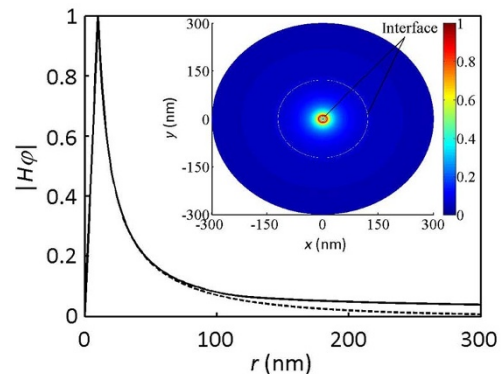


**Figure 3 | The normalised amplitude distributions of the transverse magnetic fields of the MSPPs (solid line) and SPPs (dashed line).** The MSPPs are guided by a silver nanowire placed in a silicon hole, and the SPPs are guided by a single silver nanowire. The inset (upper right) shows the transverse magnetic field in the cross-section of the waveguide for guiding the MSPPs.

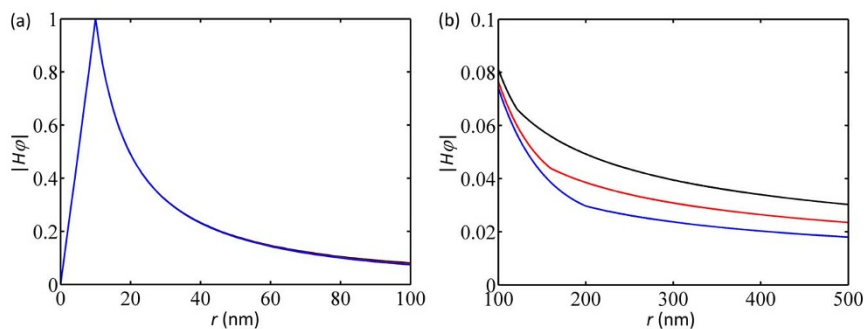


**Figure 4** | The normalised amplitude distributions of the transverse magnetic fields near (a) and distant from (b) the silver nanowire for different hole radii.

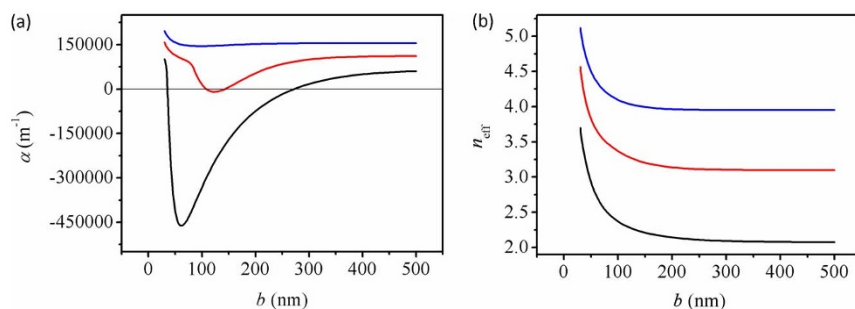


**Figure 5** | The loss coefficients (a) and effective refractive indices (b) of the MSPPs for a dielectric in the intermediate region with different permittivities.

As a result, the propagation loss decreases. When the hole radius goes to infinite, the MSPPs' field distributions tend to those of SPPs on a single silver nanowire.

When the silicon hole (with a silver wire of 20 nm radius in the centre) is filled with a dielectric with a permittivity of  $\epsilon_2 = 2$  (the black line),  $\epsilon_2 = 4$  (the red line), or  $\epsilon_2 = 6$  (the blue line), both the loss curve and the refractive index curve of the MSPPs shift up as the permittivity of the dielectric increases, as shown in Fig. 5. For  $\epsilon_2 = 2$  and  $\epsilon_2 = 4$ , parts of the curves are under the zero loss beeline, creating two zero loss hole radii. Therefore, one can obtain a long propagation distance with the MSPPs. However, the entire curve is above the zero loss beeline for the permittivity of the dielectric  $\epsilon_2 = 6$ , so there are no zero loss radii. The requirement for the existence of zero loss radii is  $\epsilon_2 < 4.05$ . When the loss coefficient  $\alpha > 0$ , we obtain that the field components are zero at infinity for all three modes, indicating they are guided modes. When the permittivity of the dielectric goes to that of silicon, the MSPPs' mode characteristics tend to those of SPPs on a silver nanowire embedded in an infinite silicon dielectric.

When a silver nanowire with a radius of  $a = 15$  nm (the black line),  $a = 20$  nm (the red line), or  $a = 25$  nm (the blue line) is placed in the centre of a glass ( $\epsilon_3 = 2.35$ ) hole, both the loss curve and the

refractive index curve of the MSPPs move up as the radius of the silver wire decreases, as shown in Fig. 6. There are also two zero loss hole radii for  $a = 20$  nm and  $a = 25$  nm, but there are no zero loss hole radii for  $a = 15$  nm. The requirement for the existence of zero loss hole radii is  $a > 19.8$  nm. When the loss coefficient  $\alpha > 0$ , the three MSPPs are also guided modes because their field components are zero at infinity. Comparing Fig. 6 with Fig. 2, one can further infer that a dielectric hole with a higher permittivity is more beneficial for maintaining low-loss MSPPs. Therefore, to attain a thinner optical beam with an equivalent propagation distance, one can simultaneously adopt a thinner metal nanowire and a higher-permittivity dielectric hole for guiding the MSPPs.

The results obtained differ from the characteristics of typical SPPs, where a trade-off is necessary between the beam width and the propagation distance. Here, this contradiction is overcome by modifying the mode fields of the SPPs. It is known that, for SPPs that propagate on a metal wire in a dielectric with a refractive index  $n_2$ , the field distribution can be modified by changing the refractive index distribution of the dielectric. For example, when a dielectric with a refractive index  $n_3$  larger than  $n_2$  is added between the metal wire and the dielectric, the field extension of the SPPs can decrease, but their

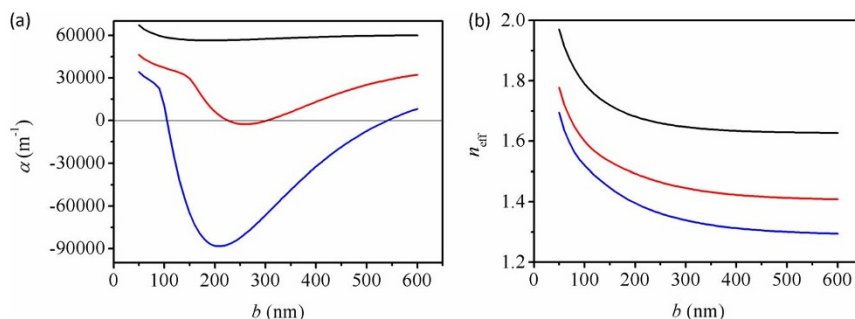


**Figure 6** | The loss coefficients (a) and effective refractive indices (b) of the MSPPs for a silver wire with different radii.



propagation loss increases<sup>32</sup>. On the contrary, by adding a dielectric with a larger refractive index outside, we significantly reduced the propagation loss largely. Under this condition, the extension of the field accordingly increases. However, as shown in Fig. 3 and Fig. 4, under an appropriate refractive index distribution, the field distribution near the metal wire changes very little, and simultaneously the extension of the field distant from the metal wire increases considerably. As a result, one can achieve both a long propagation distance and a small beam radius using MSPPs. Notably, because the field components are zero at infinity, the MSPPs are still confined modes. In fact, the nearly zero loss of the MSPPs is very similar to that of the LRSPPs. The major powers of the two modes are outside the metal, allowing them to propagate over long distances. However, the beam width of the MSPPs is much smaller than that of LRSPPs because the MSPPs have distinctive mode field distributions. Although only a small proportion of the mode's power is near the metal nanowires, the sharp mode distribution together with the long propagation distance makes the MSPPs very useful in nanophotonics, biophotonics, and integrated photonic circuits.

In conclusion, we proposed the concept of MSPPs for the nano-manipulation of optical energy. For the MSPPs, the loss coefficient goes to zero as the hole radius tends to the zero loss points. At the same time, the mode nanoconcentration can be maintained. We further presented a silver nanowire placed in a silicon hole to guide the MSPPs, and simultaneously achieved a deep sub-wavelength mode size ( $0.017\lambda$ ) and a long propagation distance (24  $\mu\text{m}$ ). The MSPPs may lead to new optical nano-manipulation methods in nanophotonics, biophotonics, and photonic circuits, which will enable a new class of optical study and applications at the nanoscale.

- Boardman, A. D. *Electromagnetic Surface Modes* (Wiley, New York, 1982).
- Raether, H. *Surface Plasmons on Smooth and Rough Surfaces and on Gratings* (Springer, Heidelberg, 1988).
- Kirchain, R. & Kimerling, L. A roadmap for nanophotonics. *Nat. Photonics* **1**, 303–304 (2007).
- Barnes, W. L., Dereux, A. & Ebbesen, T. W. Surface plasmon subwavelength optics. *Nature* **424**, 824–830 (2003).
- Maier, S. A. *et al.* Local detection of electromagnetic energy transport below the diffraction limit in metal nanoparticle plasmon waveguides. *Nat. Mater.* **2**, 229–232 (2003).
- Pile, D. F. P. & Gramotnev, D. K. Channel plasmon-polariton in a triangular groove on a metal surface. *Opt. Lett.* **29**, 1069–1071 (2004).
- Ozbay, E. Plasmonics: merging photonics and electronics at nanoscale dimensions. *Science* **311**, 189–193 (2006).
- Verhagen, E., Spasenović, M., Polman, A. & Kuipers, L. K. Nanowire plasmon excitation by adiabatic mode transformation. *Phys. Rev. Lett.* **102**, 203904 (2009).
- Gramotnev, D. K. & Bozhevolnyi, S. I. Plasmonics beyond the diffraction limit. *Nat. Photonics* **4**, 83–91 (2010).
- Stockman, M. I. Nanoplasmonics: past, present, and glimpse into future. *Opt. Express* **19**, 22029–22106 (2011).
- Sarid, D. Long-range surface-plasma waves on very thin metal films. *Phys. Rev. Lett.* **47**, 1927–1930 (1981).
- Craig, A. E., Olson, G. A. & Sarid, D. Experimental observation of the long-range surface plasmon-polariton. *Opt. Lett.* **8**, 380–382 (1983).
- Bozhevolnyi, S. I., Volkov, V. S., Devaux, E. & Ebbesen, T. W. Channel plasmon-polariton guiding by subwavelength metal grooves. *Phys. Rev. Lett.* **95**, 046802 (2005).
- Zia, R., Schuller, J. A. & Brongersma, M. L. Near-field characterization of guided polariton propagation and cutoff in surface plasmon waveguides. *Phys. Rev. B* **74**, 165415 (2006).
- Berini, P. Long-range surface plasmon polaritons. *Adv. Opt. Photonics* **1**, 484–588 (2009).
- Oulton, R. F., Sorger, V. J., Genov, D. A., Pile, D. F. P. & Zhang, X. A hybrid plasmonic waveguide for sub-wavelength confinement and long-range propagation. *Nat. Photonics* **2**, 495–500 (2008).
- Oulton, R. F., Bartal, G., Pile, D. F. P. & Zhang, X. Confinement and propagation characteristics of subwavelength plasmonic modes. *N. J. Phys.* **10**, 105018 (2008).
- Sorger, V. J. *et al.* Experimental demonstration of low-loss optical waveguiding at deep sub-wavelength scales. *Nat. Commun.* **2**, 331 (2011).
- Chen, D. Cylindrical hybrid plasmonic waveguide for subwavelength confinement of light. *Appl. Opt.* **49**, 6868–6871 (2010).
- Huang, M. H. *et al.* Room-temperature ultraviolet nanowire nanolasers. *Science* **292**, 1897–1899 (2001).
- Hill, M. T. *et al.* Lasing in metallic-coated nanocavities. *Nat. Photonics* **1**, 589–594 (2007).
- Oulton, R. F. *et al.* Plasmon lasers at deep subwavelength scale. *Nature* **461**, 629–632 (2009).
- Juan, M. L., Righini, M. & Quidant, R. Plasmon nano-optical tweezers. *Nat. Photonics* **5**, 349–356 (2011).
- Roxworthy, B. J. & Toussaint, K. C. Femtosecond-pulsed plasmonic nanotweezers. *Sci. Rep.* **2**, 660 (2012).
- Yang, H. *et al.* Protein conformational dynamics probed by single-molecule electron transfer. *Science* **302**, 262–266 (2003).
- Gerton, J. M. *et al.* Tip-enhanced fluorescence microscopy at 10 nanometer resolution. *Phys. Rev. Lett.* **93**, 180801 (2004).
- Kawata, S., Inoué, Y. & Verma, P. Plasmonics for near-field nano-imaging and superlensing. *Nat. Photonics* **3**, 388–394 (2009).
- Johnson, P. B. & Christie, R. W. Optical constants of the noble metals. *Phys. Rev. B* **6**, 4370–4379 (1972).
- Yariv, A. *Optical Electronics in Modern Communications* (Oxford U. Press, Oxford, 2007).
- Takahara, J., Yamagishi, S., Taki, H., Morimoto, A. & Kobayashi, T. Guiding of a one-dimensional optical beam with nanometer diameter. *Opt. Lett.* **22**, 475–477 (1997).
- Primak, W. Refractive index of silicon. *Appl. Opt.* **10**, 759–763 (1971).
- Goubau, G. Surface waves and their application to transmission lines. *J. Appl. Phys.* **21**, 1119–1128 (1950).

## Acknowledgments

This work is supported by the Specialized Research Fund for the Doctoral Program of Higher Education of China (Grant No. 20134408120002) and the Fund Project for Shenzhen Fundamental Research Programme (Grant No. JCYJ20130329141827934).

## Author contributions

H.L. conceived the original concept and carried out the calculations. H.L., S.R., M.Z., H.S. and I.L.L. all contributed to the writing of the manuscript.

## Additional information

**Competing financial interests:** The authors declare no competing financial interests.

**How to cite this article:** Liang, H.W., Ruan, S.C., Zhang, M., Su, H. & Li, I.L. Modified surface plasmon polaritons for the nanoconcentration and long-range propagation of optical energy. *Sci. Rep.* **4**, 5015; DOI:10.1038/srep05015 (2014).



This work is licensed under a Creative Commons Attribution-NonCommercial-ShareAlike 3.0 Unported License. The images in this article are included in the article's Creative Commons license, unless indicated otherwise in the image credit; if the image is not included under the Creative Commons license, users will need to obtain permission from the license holder in order to reproduce the image. To view a copy of this license, visit <http://creativecommons.org/licenses/by-nc-sa/3.0/>